Prediction of temperature induced defects in concrete with LS-DYNA: cement hydration implementation and applications

Mattia Bernardi[1], Fragkoulis Kanavaris[1] and Richard Sturt[1]
[1] Advanced Digital Engineering, ARUP

Abstract

The cement hydration reaction has long been recognized as an important contributor to defects throughout the service life of concrete structures.
As the hydration reaction is highly exothermic, and the thermal conductivity of concrete is relatively low, high temperatures and temperature gradients have special relevance in massive concrete structures. Massive concrete structures can endure significant cracking when temperature induced deformations are restrained. Uncontrolled cracking may compromise the structure durability and reliability, e.g. in massive concrete slabs for rail infrastructures or marine structures or the structure functionality, e.g. watertightness in liquid retaining structures or may even represent an aesthetically unacceptable defect for a concrete structure with demanding architectural finishing requirements.
The heat generation and the consequent temperature rise in concrete structures is also a problem for the damaging effects on the concrete mechanical properties following deleterious chemical reactions such as Delayed Ettringite Formation (DEF). This chemical reaction is known to be associated with thermal fields in early-age concrete usually of the order 65°C to 75°C.

Modelling such temperature effects may result in mitigation of thermal cracking and DEF in concrete. However, to include these effects in a numerical analysis of concrete structures, a special form of heat source dependent on temperature and time is required.
A novel thermal material is introduced to model the cement hydration within LS-DYNA. Three different relatively well-established hydration models were implemented and were calibrated and validated based on experimental results. The selected models were also chosen to accurately capture the thermal activation characteristics of different cement types, such as CEM I or those containing fly ash, ground granulated blast-furnace slag or limestone powder. The calibration of the models was based on isothermal and/or adiabatic calorimeter results whilst the validation was based on adiabatic and semi-adiabatic tests, as well as on comprehensive tests found in literature for given cement types. Herein two case studies where the cement hydration modelling capability in LS-DYNA was used to predict temperatures in concrete elements of considerable thickness are presented. First, the study of delayed ettringite formation and thermal cracking risk of a massive wind turbine base, then the estimation of maximum temperatures and temperature differentials during the early construction stages of a massive foundation raft on piles are presented. Insights on ongoing work and developments are given, particularly towards fully coupling thermal and mechanical analyses accounting also for concrete viscoelastic behavior, drying shrinkage, and cracking characteristics.

1 Introduction

Thermal cracking in concrete due to the exothermic reaction of cement hydration is an ongoing and well-recognized issue in concrete construction. The most efficient way to mitigate such defects is via numerical thermal analysis so that expected in-situ temperatures are calculated to determine the relevant preventive design and construction measures.

This work aims to provide a methodology to model in LS-DYNA the heat of hydration for concrete materials.

Experimentally it has been shown that the heat produced by the chemical reactions taking place in concrete during its early stages of the hydration process are a function of the degree of hydration and temperature [1].
Furthermore, following experimental evidence it is a common assumption across hydration models that the degree of hydration is itself a function of temperature and time in an integral form.

Different analytical relations are available from literature to describe the concrete heat rate of hydration. The complex relation between the heat produced during the hydration process with time and temperature have been implemented in LS-DYNA by means of a new *MAT_THERMAL_USER_DEFINED.

This work first provides a brief presentation of the three implemented thermal material models. Then, two project applications are described as an application of this new LS-DYNA thermal material`s capability. A methodology is provided to calibrate the different cement hydration thermal materials against experimental data. Finally, more details are provided on how the pouring sequence was modelled by means of a “staged thermal analysis” that includes time varying thermal conductivities and time varying thermal boundary conditions.

2 Cement heat of hydration thermal material models

2.1 Klemczak and Knoppik-Wrobel model [2]

This model is the most basic hydration model of the three implemented. It has been considered due to its simplicity of calibration, but it may be expected to be the less accurate than other considered models as calibration of its parameters against experimental data can achieve only limited accuracy. Using this model, the time and temperature dependent heat of hydration Q is calculated as:

$$Q(t,T) = Q_{pot} \cdot \exp(-a \cdot t_e^{-0.5}) \qquad \text{Eq. (1)}$$

with $a = a_6 \cdot t_e^{a_7}$ where a_6 and a_7 are fitting parameters.

where

Q_{pot} = potential/maximum heat of hydration [kJ/kg]
t_e = Arrhenius equivalent age [seconds or days]

The Arrhenius equivalent age is used to take into account the temperature sensitivity of the cement hydration and is expressed as:

$$t_e(t,T) = \int_0^t \exp\left[-\frac{E_a}{R}\left(\frac{1}{T} - \frac{1}{T_{ref}}\right)\right] dt \qquad \text{Eq. (2)}$$

where

E_a = Mix-dependent activation energy [J/mol]
R = Universal gas constant [J/Kmol]
T = Temperature of concrete at time t [°C]
T_{ref} = Reference concrete temperature. Taken as 20 °C

2.2 Jonasson model [3]

This model can more accurately represent the development of cement heat of hydration than the Klemczak and Knoppik-Wrobel model [2].

$$Q(t,T) = Q_{pot} \cdot \exp\left(b \cdot \ln(1 + \frac{t_e}{\tau_k})^a\right) \qquad \text{Eq. (3)}$$

with a, b and τ_k being fitting parameters.

Q_{pot} and t_e are as defined in the previous paragraph 2.1.

2.3 Reinhardt model [1]

This model is perhaps the most comprehensive amongst those herein considered and can achieve the most accurate results following calibration against experimental tests. However, it can be more demanding in terms of calibration efforts. First, the Reinhardt model requires a set of input scalars and a curve (the normalised heat generation rate) to be fitted to experimental data. Furthermore, the normalised heat generation rate would ideally be calibrated against a series of isothermal calorimeter tests results. On the other hand, the previous two hydration models are a function of input scalar quantities only (no input curves required) and may be calibrated by means of a single adiabatic test of the cement mix considered or also using isothermal calorimeter results.

$$\dot{Q}(t,T) = f(\alpha) \cdot A_t \cdot \exp\left(-\frac{-E_a}{RT}\cdot\right) \quad \text{Eq. (4)}$$

with

$f(\alpha)$ being the normalised heat generation rate,

$$\alpha = \frac{Q(t)}{Q_{pot}} = \frac{\text{amount of cement that has reacted at time t}}{\text{total amount of cement at time t=0}} \text{ the degree of hydration,} \quad \text{Eq. (5)}$$

A_t is the rate constant.

E_a, R and T are the activation energy, universal gas constant and curing temperature, respectively. More information about this model can be found in Azenha [4].

Two project applications of concrete heat of hydration modelling are described in the following sections.

3 Case study 1: thermal analysis of a wind turbine concrete foundation

This first work consisted in the thermal analysis of an existing wind turbine concrete foundation which exhibited cracking. The scope of the work is to check whether cracking occurrence in the foundation was caused by Delayed Ettringite Formation (DEF), i.e., whether the initiation temperature for DEF is likely to have been exceeded.

A numerical model of the wind turbine foundation was developed in LS-DYNA to analyze the temperature distribution over time and maximum temperatures that may have been developed in the foundation structure during the early age of concrete hardening. That is, from the end of concrete casting to the first few days/weeks after pouring when the peak temperature and temperature gradients are reached.

3.1 Thermal material calibration for the Reinhardt model

The concrete mix used for the wind turbine foundation is “CEM II A L 42.5R”. The set of material input parameters required for the Reinhardt model to fit experimental tests carried out for this cement mix were readily available in [4]. A summary of a calibration procedure for the Reinhardt model consistently with [4] is herein reported for reference.
As described in Eq. 4 of section 2.3 one of the main assumptions of the Reinhardt model is that the heat evolution can be split into two independent parts: one depending on the degree of reaction only and the other depending on the temperature (ref. [1]).

In order to make best use of the independence of the degree of hydration from temperature a series of isothermal colorimeter test are recommended so that for each test the normalised heat generation rate can be explicitly measured as $f(\alpha) = \frac{\dot{Q}(\alpha)}{\dot{Q}_{max}(\alpha)}$, with α also explicitly defined and measured over the course of the isothermal tests as the ratio of the heat released at time “t” and the maximum heat released during the entire course of the test: $\alpha = \frac{Q(t)}{Q_{max}}$ (ref. Eq. (5)).
The activation energy E_a and A_t can be readily obtained by measuring the heat generation rate $\dot{Q}$ and the temperature in isothermal tests carried out at different temperatures. Taking the natural logarithm of

Eq. (4), the natural logarithm of the heat rate becomes linearly correlated to the inverse of temperature: $\ln(\dot{Q}) = m \cdot \frac{1}{T} + b$.

E_a and A_t can be directly computed as $E_a = R \cdot m$ and $A_t = \frac{e^b}{f(\alpha)}$.
It is recommended (ref. [5]) that the parameters of Eq. (4) used to compute E_a and A_t across the different isothermal tests, are evaluated when the heat generation rate $\dot{Q}$ is at its maximum (i.e. for $f(\alpha) = 1$).

3.2 Thermal modelling of the wind turbine concrete foundation

The objective of the analysis is to accurately predict the peak temperature and temperature gradient across the different parts of the concrete foundations. These two measures directly relate to Delayed Ettringite Formation (DEF) and more generally cracking induced by constraint of deformation induced by thermal strains.

To correctly capture the heat development and heat flow within the concrete structure a “staged” thermal analysis is carried out. Here, when a new concrete batch is cast, both boundary conditions and thermal material properties are changed to reflect the “new added” material at each stage of the pouring sequence.

Figure 1 shows how only a 22.5° slice of the rounded foundation has been modelled taking advantage of the axial symmetry of the structure.
During the first stage of pouring the concrete on the main core and fins of the foundation, together with the central steel member (ref. Figure 1) are not yet cast.
That is modelled in the analysis by scaling the thermal conductivity of the material yet to be cast to zero and applying the appropriate convective boundary conditions on the set of elements at the top of the slab.
During “stage 2” the dormant elements (concrete “fin” and main core casting) will retain the applied initial temperature and won`t be subjected to any heat flux.

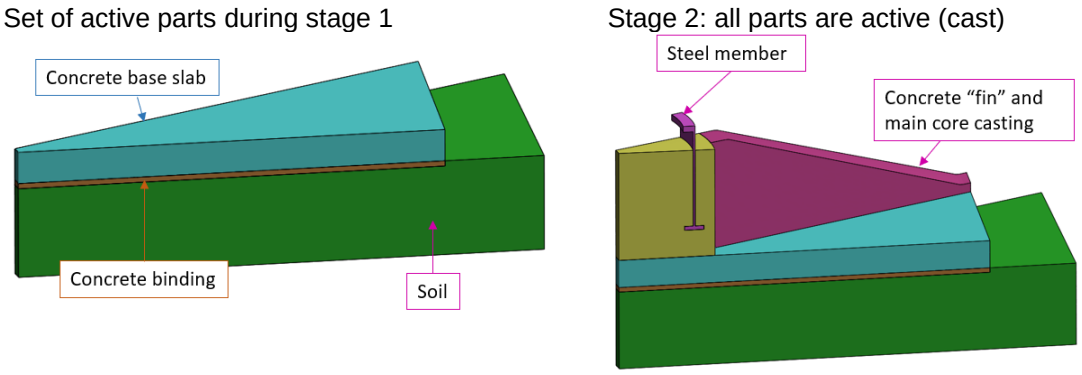

Figure 1: on the right the set of “active” elements at the start of the analysis (stage1), on the left the set of active elements from the start of stage 2 to the end of the analysis.

Figure 2, on the left shows the temperature distribution at the start of the analysis. Dormant parts are greyed out in transparency. The soil temperature is 16° Celsius whilst the concrete casting temperature is 25.4°. Ten hours after casting the central part of the concrete slab reaches the peak temperature of 53.6°.

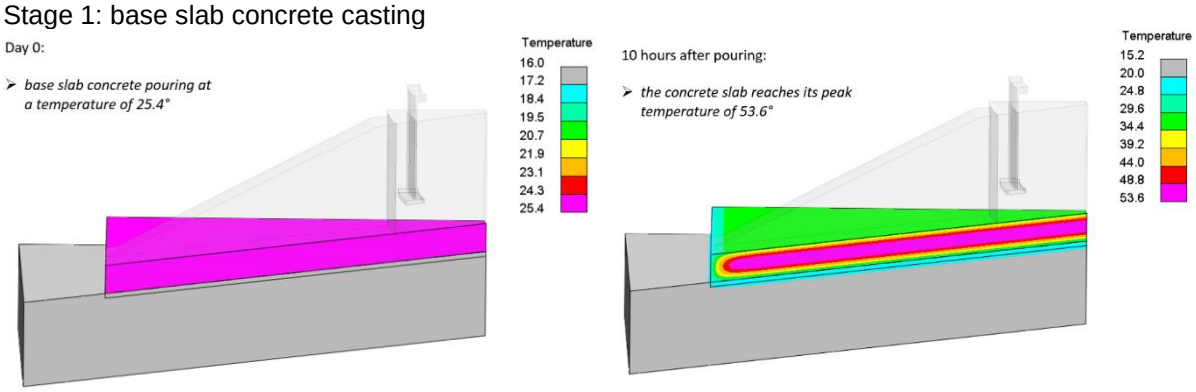

Figure 2: temperature distribution across the soil and the concrete slab at the start of the analysis and 10 hours after pouring when the peak temperature is reached at the centre of the slab.

Figure 3 shows the temperature distribution at the start of stage 2 on the left, that is 14 days after the concrete slab was poured. The temperature distribution 12 hours and 24 hours after the beginning of stage 2 are shown respectively on the right and at the bottom of Figure 3. The latter two plots capture the state in time when the fin and the main core reach the peak temperature over the course of the analysis.
In this case heat is dissipated both through the top convective boundary condition but also through the thermal contact of the concrete core and “fin” to the bottom slab, hence through the soil.

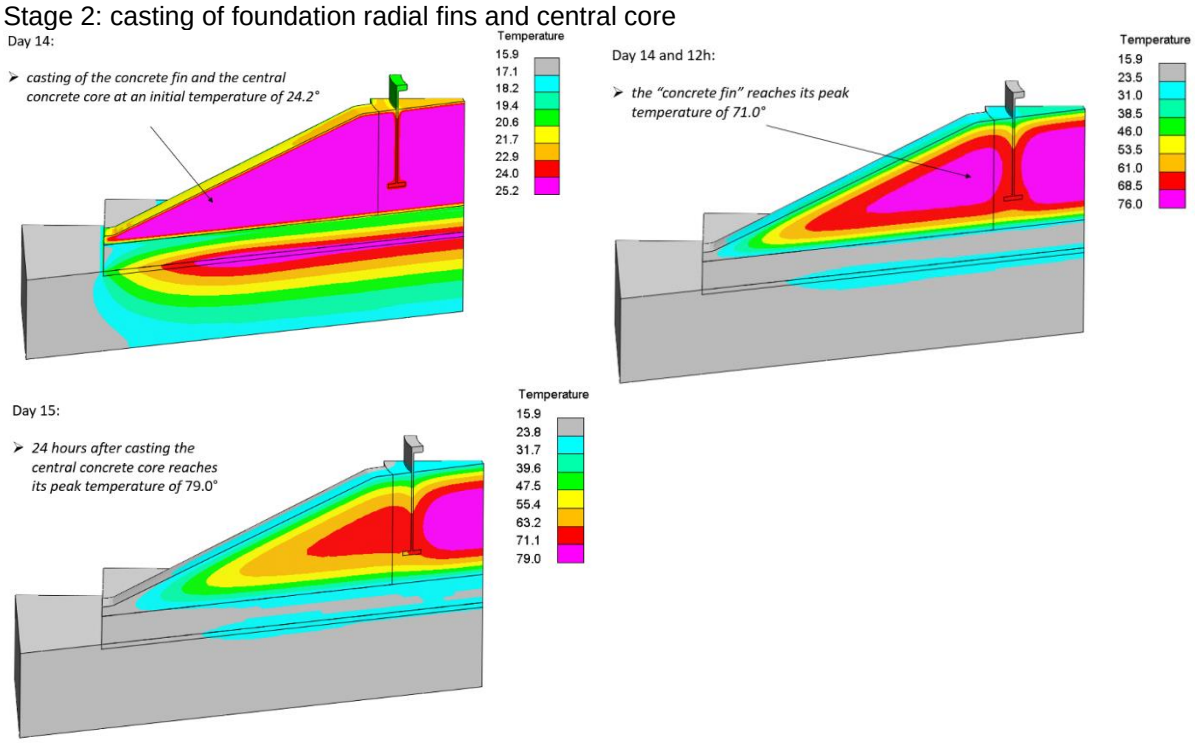

Figure 3: temperature distribution across the full concrete foundation at the start of stage 2, 12 hours, and 24 hours after the beginning of stage two, when the peak temperature in the concrete “fin” and in the concrete core is reached.

Figure 4 shows the temperature-time history at the points where the peak temperature is reached within the base slab, the main core and concrete fin. As per the graph, the heat developed within the concrete slab is mostly dissipated by convection before casting of the upper part (within the first 14 days), whilst after casting of the main core and the top fin, the peak temperature on the center of the slab increases again following the top new cast concrete heat source and does not significantly drop even after 50 days. Although within this analysis, that is not affecting the peak temperature of the cast elements, that

is showing how important it is to provide a sufficiently large time interval between consecutive casting stages. That is particularly important for thicker concrete component cast within the ground which provides a relatively good insulation. The ground insulation together with either a large member thickness or the insulation provided by adjacent existing concrete may drastically increase the time required for one element to dissipate its heat of hydration.
The developed thermal material model, together with LS-DYNA transient thermal analysis capabilities can allow for an accurate prediction of how the temperature field varies in time as a function of the different structural design parameters, e.g. pouring sequence, time between pouring stages and size of the pours.

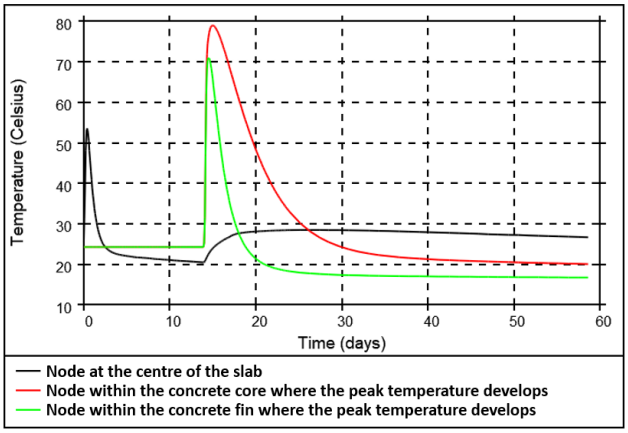

Figure 4: temperature time history at the three points where the peak temperature is reached within the base slab, the main core and concrete fin.

4 Case study 2: thermal analysis of a massive foundation raft

Similarly to case study 1, the scope of this 2nd case pertained to the estimation of maximum temperatures and temperature differentials to avoid Delayed Ettringite Formation (DEF) and prevent thermal cracking following the development of heat of hydration within early-age concrete. A series of thermal analyses were carried out for all reinforced concrete elements more than 1m thick from a large rail track foundation structure.

Figure 5 shows a cross section of the different elements analyzed. The typical model set up and some results from the base slab and capping slab simulations are described in section 4.2 as examples of typical concrete component thermal analyses.

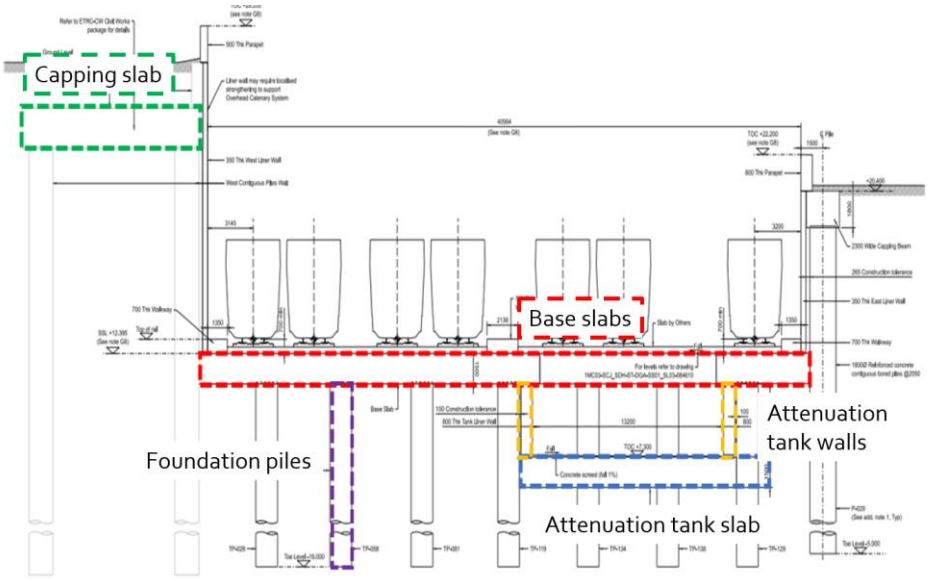

Figure 5: Thick concrete elements relevant to the temperature control plan

The analyses consider two sets of simulations: one for winter and one for summer conditions, where different casting temperature (concrete initial temperature) and ambient temperature (soil and unreactive concrete initial temperature, and ambient temperature for convective boundary conditions) are considered.

Furthermore, for both summer and winter conditions, four different cement mixes are analyzed. These are defined by durability requirements and selected to minimize the carbon footprint of the concrete mix (ref. [6]). The LS-DYNA thermal analyses are carried out with Jonasson's cement hydration model.
Table 1 reports the cement hydration model input parameters (cement content, potential heat of hydration Q_{pot}, and reference concrete temperature T_{ref}), and the parameters calibrated from the available adiabatic test experimental data: a, b and τ_k. Further detail on the calibration of a, b and τ_k are provided in the next section 4.1. The discrepancies between model input parameters for different supplementary cementitious materials in Table 1 stems from differences in hydration reaction kinetics and evolution of hydration in each combination (Portland cement + GGBS or fly ash). However, it is noted how α, b, and τ_k are curve fitting parameters and do not strictly relate to any physical interpretation. Large positive values of τ_k can be associated to a time delay in time the hydration process, similarly larger negative value of b also represent a slower hydration process, conversely larger negative values of α correspond to an increase in the speed of the hydration process. Hence, comparable results may be obtained with very different α, b and τ_k calibration parameters.

Table 1: Hydration model parameters for cement types considered in the analysis

Cement mix	Cement content [kg/m3]	Q_{pot} [J/kg]	α	b	τ_k [s]	T_{ref} [deg Celsius]
30% Fly ash	431	281000	-0.50	-0.05	20000000	20
35% GGBS*	432	325000	-2.05	-8.00	6000	20
50% GGBS*	452	270000	-2.05	-8.00	6000	20
70% GGBS*	464	230000	-2.05	-8.00	6000	20

*GGBS : Ground Granulated Blast-furnace Slag

4.1 Thermal material calibration for the Jonasson model

The transient thermal analysis is conducted with LS-DYNA which employs Jonasson's cement hydration model [3] as already defined in section 2.2 Eq. 3.

As concerns the calibration of a, b and τ_k particular attention is paid to minimizing the error between the adopted Jonasson model and the experimental results around two days after pouring. That was done to reliably model the peak temperature and temperature differential reached in the structural elements. The estimated peak temperature is reached between 1.5 and 2.5 days after casting on all analyzed elements (ref. slabs, walls, piles etc.).

Matching the heat of hydration at about 2 days after casting may lead to overestimating the produced heat after the peak is reached: e.g. after 1week or more. That may be a potential limitation of the Jonasson model. However, in general the peak temperature and the maximum temperature differential are not sensitive to the extra heat produced in the long term as peaks are reached within the first few days after casting, and after that the temperature is cooling to ambient regardless.

Finally, it was checked that the "additional" heat produced in the long term within the simulation, e.g. longer than 3 days since casting, does not affect the peak temperature in the subsequent/adjacent pours. It is confirmed that the temperature profile time history only changes locally at the boundaries between adjacent pours, and that is not sufficient to change the peak temperature and peak temperature gradients which occurs at the center of each new pour.

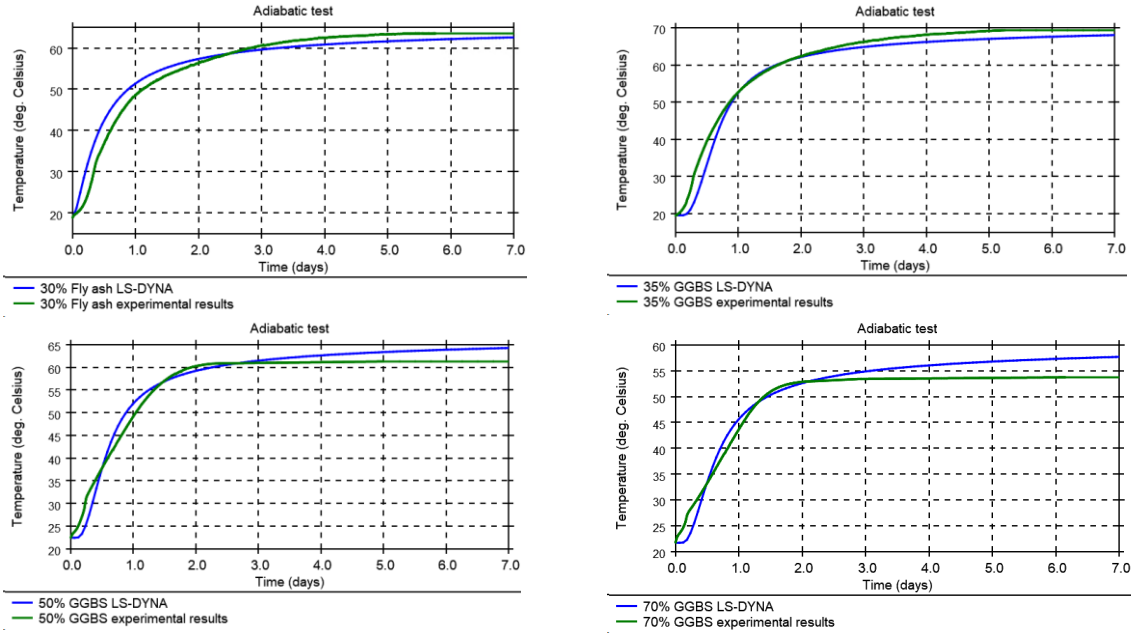

Figure 6: model calibration curves for adiabatic tests for cement mixes: 30% Fly ash, 35%, 50% and 70% GGBS

4.2 Thermal analysis model set up and review of results

The transient thermal analysis of the base slab considers four pouring stages. Similarly to the wind turbine concrete foundation, the thermal conductivity of the dormant parts is set to zero before casting and changed to the appropriate value only once the part is casted. Convective boundary conditions are also varied over time to reflect surfaces which are exposed to the ambient air before the concrete is casted. The convection heat transfer coefficient is changed to zero on surfaces where concrete is poured, only after concrete is casted (ref. Figure 7).

The analysis considers four consecutive pours. The concrete is surrounded by air at the top (convective boundary conditions), and soil and unreactive concrete at the bottom and at the sides. Concrete is deemed to be "unreactive" when it is in thermal equilibrium with the ambient temperature and hydration processes have completed: e.g., casting of the "non-reactive" concrete occurred months before casting of the reactive concrete such as the considered slab.

Figure 8 shows a typical analysis output: the temperature distribution across the three active concrete pours at the point in time when the maximum temperature is reached in the third pour.

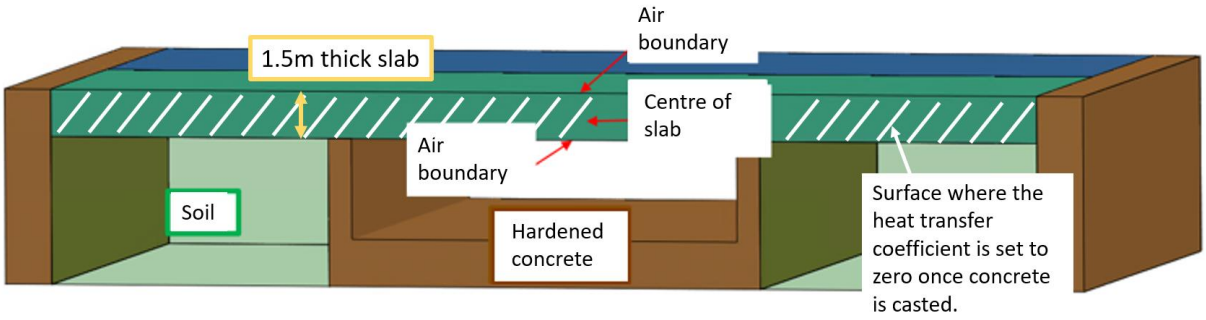

Figure 7: model set up for the analysis of the base slab

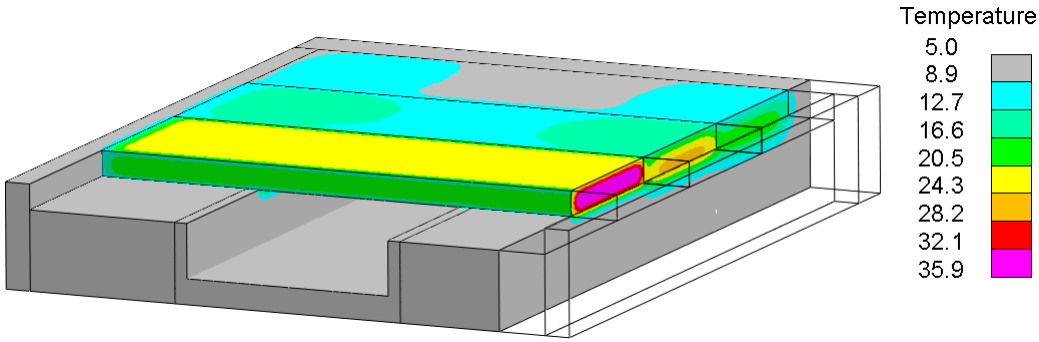

Figure 8: temperature contour plot of the base slab when the peak temperature is reached in the third pour. Winter ambient conditions with a 50% GGBS cement mix are considered.

Figure 9 shows in purple the temperature time histories at the center of the three pours where the peak temperature is reached. The curves in green show the peak temperature time histories for each of the three pours on the external surfaces. Thus, the purple curves maximum value is the peak temperature reached at each pour, whilst the maximum difference between the green and the purple curves is the maximum temperature differential.
The three different pours show the same peak temperature and temperature differential time histories. That is, the time interval between pours is sufficient for the heat within each pour not to increase the peak temperature in the following pour.

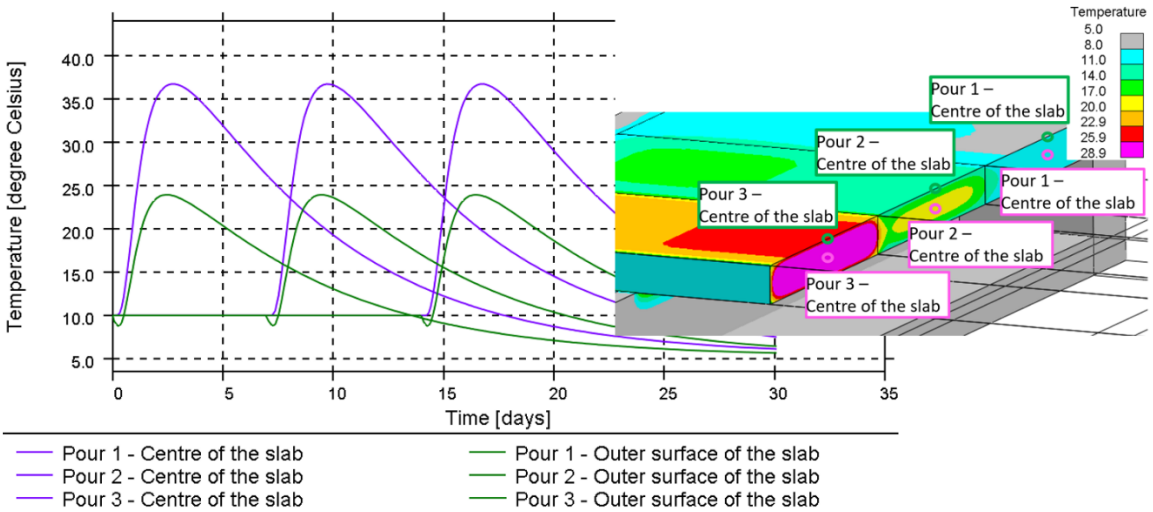

Figure 9: temperature time history at the center and at the side of each of the three pours within the analyzed sequence.

In this regard it is noted how there always is a region within the new pour (adjacent to the previous pour) in which the temperature is increased because of the heat flow from the previous pour. If the time interval between consecutive pours is sufficiently close to the point in time when the maximum temperature is reached, this region may become sufficiently large to increase the maximum temperature and

temperature gradient of the newly cast pour (i.e. width of pour affected by the previous pour temperature equal to half the pour width). That may result in damaging effects as each new pour would show a higher peak temperature and temperature gradient than the previous one.

Figure 10 and Figure 11 show how temperature time histories are affected by the time scale of the pouring sequence in the capping slab during summer conditions. The green curves of Figure 11 correspond to 2 points very close to the boundary between pours (0.25m). Here the continuous curve (first pour being cast) undergoes an increase in temperature after 7 days when the second pour is added. However, this increase in temperature never exceeds the peak temperature reached during casting of the first pour alone. This increase in temperature is no longer visible at a distance of 1.25m from the pour's boundary (ref. light blue and black curves in Figure 11). That is, the first pour heat affects the second pour temperature time histories only for a width of less than 1.25m, and this correlation between subsequent pours is not sufficient to increase the peak temperature and temperature gradient across the whole length of the pour. That would not be the case for shorter intervals between consecutive pours.

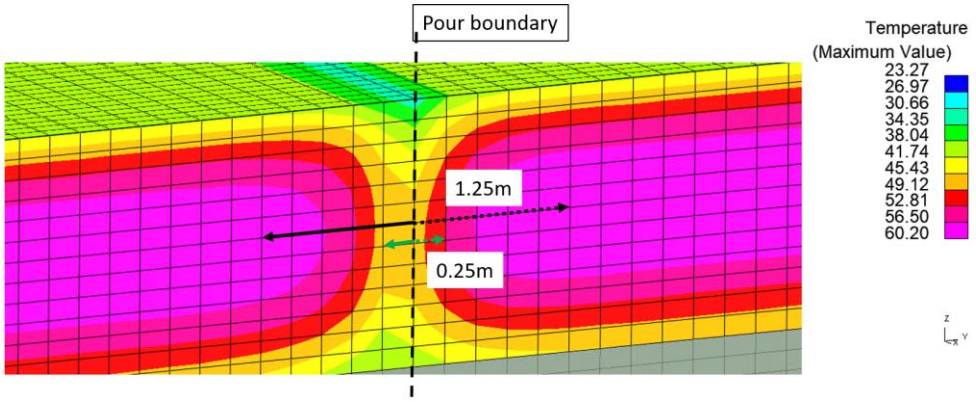

Figure 10: contour plot of the maximum temperature at the boundaries between two consecutive pours in the capping slab during summer conditions.

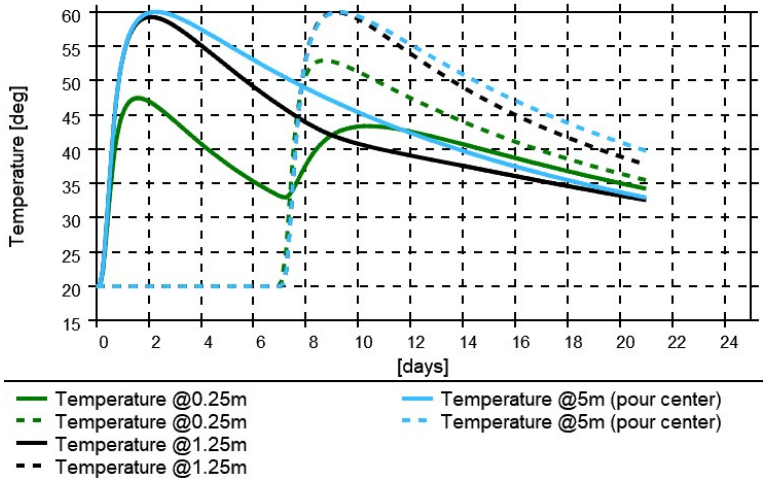

Figure 11: temperature time history at six different gauge points on two adjacent pours: two points at 0.25m from the pour boundary, two points at 1.27m from pour boundary and two at mid-pours (5m from boundary).

5 Conclusions

A novel *MAT_THERMAL_USER_DEFINED is written within LS-DYNA to model the cement hydration. Three different relatively well-established hydration models are implemented and described.

Two case studies where the cement hydration modelling capability is used to predict peak temperatures and temperature gradients in concrete elements of considerable thickness (i.e. greater then 1m) are presented. The first case study pertains to modelling of a massive wind turbine base, the second regards modelling of massive foundation rafts. Here more details are provided on the heat of hydration material model calibration and how staged thermal analyses are carried out to correctly capture the varying boundary conditions following casting of a new pour.

Further work is being carried out to perform a fully coupled thermo-mechanical analysis where the evolving mechanical properties of concrete, e.g. ageing concrete with time-varying stiffness, are accounted for, together with a concrete viscoelastic constitutive behavior (creep) and shrinkage strains. Note how these phenomena are most relevant in early age concrete, i.e. during the same period when heat of hydration effects are most significant (when peak temperature and temperature gradient are reached).

As defined in [7], we would first aim to be able to assess cracking risk. That may be achieved by means of a simplified fully coupled thermo-mechanical analysis of concrete structures where cracking and reinforcement effects are neglected, concrete is modelled as viscoelastic with ageing material properties, and thermal and shrinkage strain are included. Here the sought output is the cracking index, expressed as the ratio of simulated tensile stress to the tensile strength capacity at a particular time instant. If the cracking risk is high, then some cracking will probably be occurring; this simulation type would focus on pre-cracking stages and disregard local cracking in stress singular points around notches, openings or local forces.

In a second stage we aim to extend this thermo-mechanical analysis of concrete structures to a non-linear concrete material. Reinforcement may be accounted for explicitly aiming for crack width control outputs and prediction of stresses redistribution following the non-linear response of reinforced concrete after cracking.

6 Literature

[1] Reinhardt. Temperature development in concrete structures taking account of state dependent properities. Int. Conf. Concrete at Early Ages, Paris, France (1982).

[2] B. Klemczak, A. J. "Analysis of Early-Age Thermal and Shrinkage Stresses in Reinforced Concrete Walls." ACI Structural Journal (2014).

[3] Jonasson, J.-E. Modelling of Temperature, Moisture and Stresses in Young Concrete. Doctoral Thesis, Lulea University of Technology, Lulea (1994).

[4] Azenha, M. A. "Numerical simulation of the structural behaviour of concrete since its early ages." Doctoral Thesis, University of Porto (2009).

[5] Wadso L., “An experimental comparison between isothermal calorimetry, semi-adiabatic”, Nordtest report TR 522 (2003).

[6] Mineral Product Association, “Embodied CO2e of UK cement, additions and cementitious material”, Fact Sheet 18 available at: “https://cement.mineralproducts.org/documents/Factsheet_18.pdf”.

[7] Azenha, M., Kanavaris, F., Schlicke, D. et al. Recommendations of RILEM TC 287-CCS: thermo-chemo-mechanical modelling of massive concrete structures towards cracking risk assessment. Mater Struct 54, 135 (2021)